discontinuity will appear automatically. In the case of $a(0)=C_1/C_2$, a weak wave will stabilize as a wave of constant amplitude. From Eq. (20) we have

$$\frac{dS_c}{dC_1}=\frac{1}{C_1}\left\{\frac{\exp(C_1S_c)}{a(0)C_2}-S_c\right\}>0$$

which implies that the effect of radiative heat transfer will delay shock formation.

Acknowledgment

The work is supported by the University Grants Commission under the project "Non-linear Wave Propagation in High Temperature Phenomena."

References

[1] Becker, E., "Relaxation Effects in Gas Dynamics," *Aeronautical Journal*, Vol. 74, 1970, pp. 736-748.

[2] Bowen, R. M. and Chen, P. J., "Some Comments on the Behavior of Acceleration Waves of Arbitrary Shape," *Journal of Mathematical Physics*, Vol. 13, 1972, pp. 958-960.

[3] Ram, R. and Srinivasan, S., "Propagation of Sonic Waves in Radiating Gases," *Zeitschrift für angewandte Mathematik und Mechanik*, Vol. 57, 1977, pp. 191-193.

[4] Jeffrey, A., "The Development of Jump Discontinuities in Nonlinear Hyperbolic Systems of Equations in Two Independent Variables," *Archive for Rational Mechanics and Analysis*, Vol. 14, 1963, pp. 27-37.

[5] Suhubi, E. S. and Jeffrey, A., "Propagation of Weak Discontinuities in a Layered Hyperelastic Half-Space," *Proceedings of the Royal Society of Edinburgh*, Vo. 75, 1976, pp. 209-221.

[6] Varley, E., "Acceleration Fronts in Viscoelastic Materials," *Archive for Rational Mechanics and Analysis*, Vol 19, 1965, pp. 215-225.

[7] Green, W. A., "The Growth of Plane Discontinuities Propagating in a Homogeneously Deformed Materials," *Archive for Rational Mechanics and Analysis*, Vol. 16, 1964, pp. 79-88.

[8] Collins, W. D., "One Dimensional Nonlinear Wave Propagation in Incompressible Elastic Materials," *Quarterly Journal of Mechanics and Applied Mathematics*, Vol. 19, 1966, pp. 259-328.

[9] Ram, R. and Pandey, B. D., "On the Growth and Decay of Acceleration Waves in Transient Gas Flows with Vibrational Relaxation," *Acta Mechanica*, Vol. 33, 1979, pp. 171-178.

[10] Olfe, D. B., *Radiation and Re-entry*, Academic Press, New York, N.Y., 1968.

J80-163

Single Pulse Laser Irradiation of Fiberglass

30012

60002

Peter K. Wu* and Robert G. Root* 90003

Physical Sciences Inc., Woburn, Mass.

Introduction

THE phenomenology associated with high-power laser irradiation of materials has been of interest for many years.[1-3] This Note will introduce the concept of "residual energy" in a laser irradiated material and examine its effect on the mass removed from a fiberglass surface by pulsed laser radiation. The accumulation of the "residual energy," which is defined as that portion of pulse energy remaining in the material after the termination of the laser pulse, is expected to pyrolyze the resin (with a pyrolysis temperature of approximately 900 K) which binds the plies of glass fibers that form fiberglass. In addition, as the laser pulse fluence increases, the in-depth vaporization of fiberglass limits the magnitude of the residual energy useful for potential multiple pulse mass removal mechanisms.

Analysis

A one-dimensional transient heat conduction analysis with in-depth absorption of laser radiation has been formulated for fiberglass composites, and the governing equation can be written as

$$\rho C_p\frac{\partial T}{\partial t}=\frac{\partial}{\partial x}\left(K\frac{\partial T}{\partial x}\right)+(C_p)_r\frac{\partial}{\partial x}[\dot{m}_r(x)T]+\phi_r\omega_r+\Delta H\omega-\frac{\partial I}{\partial x} \tag{1}$$

where ρ is the density of the solid; C_p is the specific heat of the solid; T is the temperature; K is the thermal conductivity; $(C_p)_r$ is the specific heat of the resin gas; $\dot{m}_r$ is the mass flux of the resin gas; ϕ_r is the enthalpy of pyrolysis per unit mass of gas generated; ω_r is the rate of gas generation per unit volume; ΔH is the heat of vaporization of solid; ω is the vaporization rate per unit volume; I is the absorbed laser intensity; and t and x are the time and axial coordinates, respectively. For the radiative source term, it is assumed that $I=I_0e^{-\tau}$, where I_0 is the initial laser intensity (at $x=0$); τ is the optical depth defined as[4]

$$\tau=\int_0^x K_v\,dx$$

and the absoption coefficient K_v is assumed to scale as the solid density. Equation (1) has been solved by an explicit forward-marching technique in finite difference form with an initial condition $T(x,t=0)=T_0(x)$ and the boundary conditions for $t>0$

$$-K\frac{\partial T}{\partial x}=I_0[1-\exp(-K_v\Delta x/2)]+(C_p)_r\dot{m}_rDT+\phi_r\omega_r\Delta x/2-\dot{m}\Delta H-\epsilon\sigma T^4-\frac{\rho C_p\Delta T}{\Delta t}\frac{\Delta X}{2},\quad x=0$$

$$\frac{\partial T}{\partial x}=0,\quad x=L$$

where $\dot{m}$ is the vaporization rate at the surface; ϵ is the emissivity; σ is the Stefan-Boltzmann constant; and L is the wall thickness. The pyrolysis rate is adopted from Ref. 5.

$$\omega_r=-\rho_r^3[1.39\times10^{-9}\exp(-20440/T)+11570\exp(-8556/T)]$$

where ρ_r is the resin density. Expressions for ρ_r and $\dot{m}_r$ are given in Ref. 3.

For surface temperatures well above the normal boiling point, the surface pressure p_s is given approximately by $P_s\approx\rho_va^2$, where ρ_v is the vapor density and a is the sonic velocity of the escaping vapor. But, P_s as a function of T can be approximated by

$$P_s=P_0e^{-\Delta H/RT}$$

where p_0 is a constant which can be determined from the normal boiling point, and R is the ideal gas constant. With the sonic velocity given by $a=\sqrt{\gamma RT}$, where γ is the ratio of specific heats, the vaporization rate at the surface becomes

$$\dot{m}\approx p_0e^{-\Delta H/RT}/\sqrt{\gamma RT}$$

Received Sept. 10, 1979; revision received Nov. 30, 1979.

Index categories: Lasers; Combustion in Heterogeneous Media; Heat Conduction.

*Principal Scientist. Member AIAA.

In formulating this model, we have assumed that in-depth vaporization of glass fibers (at about 3100 K) as well as in-depth pyrolysis of resin (at about 900 K) takes place, and the resultant gases are assumed to be able to escape through the porous char. Now, Eq. (1) can be solved with the appropriate initial and boundary conditions to provide complete temperature and density profiles in the solid along with the residual energy. In the following calculations, the thermodynamic properties of fiberglass are taken from Ref. 6.

The Residual Energy

Fiberglass is constructed by binding many plies together by resin which has a rather low pyrolysis temperature (approximately 900 K), and each ply has a thickness of about 0.025 cm. When a surface of fiberglass is irradiated by a repetitively pulsed laser, the plies can be loosened (and perhaps removed) by pyrolyzing a major portion of the resin in the interface between plies. The accumulation of residual energy Q_r, which, as previously indicated is defined as that portion of the pulse energy remaining in the solid after the termination of the laser pulse, can raise the temperature at the interface between the first two plies, after a train of pulses, to about 900 K. Significant resin is then pyrolyzed, i.e., 50%. Here, we will use the preceding analysis to calculate the residual energy and indicate its possible effect on ply removal.

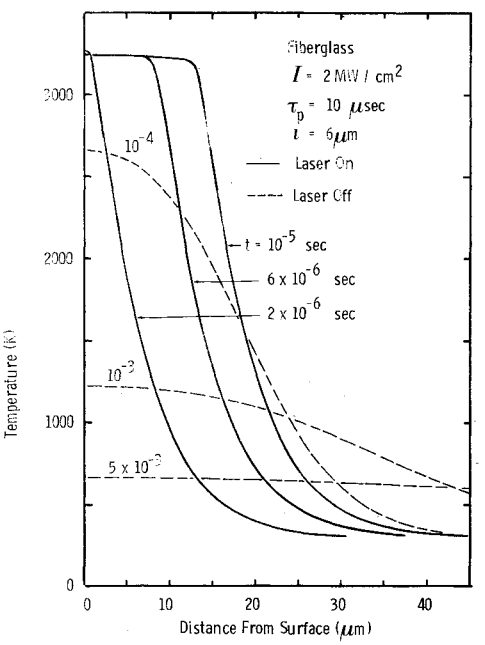

Fig. 1 Temperature distributions at various times.

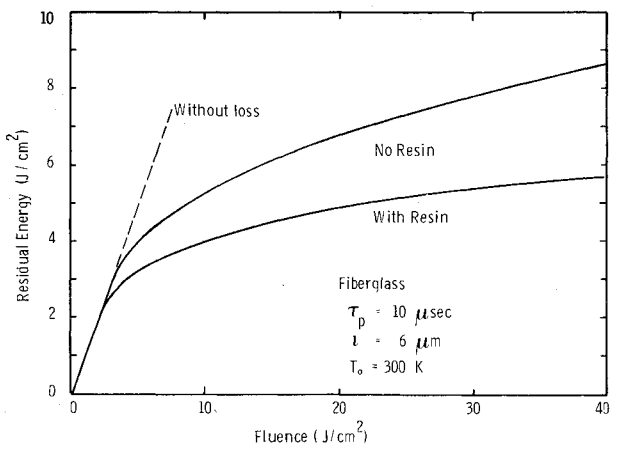

Fig. 2 Residual energy as a function of fluence.

Results and Discussion

Calculations have been carried out for pulse times of 10, 20, and 40 μs at various intensities. A nominal absorption length for 10.6-μm laser radiation in fiberglass has been shown to be approximately 6 μm,[7] and the sensitivity of the residual energy to the uncertainty in the absorption length will be later assessed. Shown in Fig. 1 are some typical temperature distributions at various times for the case of absorbed intensity $I = 2$ MW/cm^2 pulse time $\tau_p = 10$ μs, absorption length of 6 μm, and an initial temperature of 300 K. The solid lines are the temperature profile during the laser pulse, and the dashed lines are the temperature distributions after the termination of the laser pulse. The flat top feature of the temperature profile is due primarily to the in-depth vaporization of fiberglass which is one of the important factors limiting the magnitude of the residual energy as the pulse energy increases. In the calculations, we vary both intensity and pulse time, and the results show that the residual energy is primarily a function of fluence. The residual energy vs fluence is given in Fig. 2 for the case of $\tau_p = 10$ μs, $\ell = 6$ μm, and $T_0 = 300$ K. Without losses to pyrolysis of resin and/or vaporization of fiberglass, the residual energy is simply the absorbed fluence, i.e., for fluences less than 3 J/cm^2. However, as the fluence increases to about 3 J/cm^3, the residual energy increases significantly slower. For the case of virgin fiberglass encountered by the first pulse (lower curve), the residual energy is about 4 J/cm^2 at an incident fluence of 10 J/cm^2, while it increases to 5.7 J/cm^2 at 40 J/cm^2 incident. When the resin has been completely removed, the residual energy increases by about 25% at incident fluence $F = 10$ J/cm^2 and 50% at $F = 40$ J/cm^2 (upper curve). In the above calculations, the absorption length of 6 μm and the initial temperature of 300 K have been used. However, there is uncertainty in the absorption length,[7] and the initial temperature for each pulse increases in subsequent pulses due to the accumulation of residual energy. The effects of absorption length and initial temperature on the residual energy are shown in Fig. 3 for the case of $I = 2$ MW/cm^2 and $\tau_p = 10$ μs. The dashed line shows the effects of absorption length. The residual energy increases from about 3-6.5 J/cm^2 when the absorption length varies from 2-10 μm, and it drops to about 0.2 J/cm^2 for surface absorption. The effects of initial temperature on Q_r are shown by the solid lines (i.e., both with and without resin), and Q_r decreases with increasing T_0. For T_0 greater than approximately 900 K, the upper curve should be used because the resin would be pyrolyzed even without laser radiation.

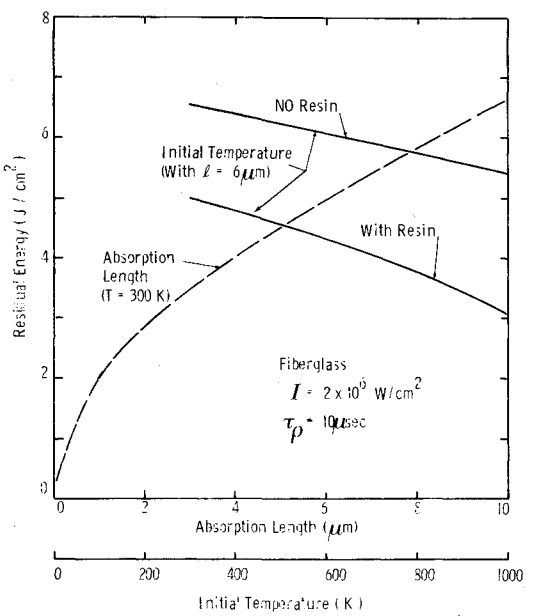

Fig. 3 Effects of absorption length and initial temperature on residual energy.

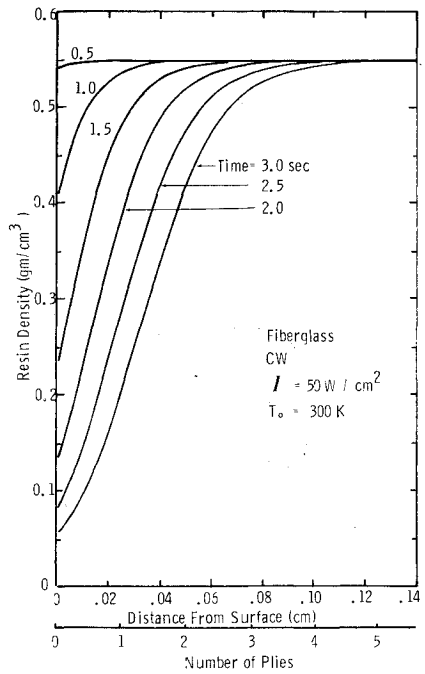

Fig. 4 Resin density distributions at various times for an equivalent cw laser.

As shown in Fig. 2, a residual energy of 5 J/cm^2 can be deposited in fiberglass with pulse fluence of $F \simeq 8$ J/cm^2 (without resin) and $F \simeq 20$ J/cm^2 (with resin). Let's consider a 10-pps pulsed laser which delivers an average residual energy of 5 J/cm^2 per pulse. The average intensity for an equivalent CW laser is 50 W/cm^2. With an average intensity of 50 W/cm^2, the one-dimensional heat conduction analysis provides the temperature and density history. As shown in Fig. 4, the resin density profiles are given at various times. At the time of about 2.5 s, the resin content at the interface between the first two plies has been reduced by a factor of 2. Hence, if this criterion is used for ply removal, it is possible to remove the first ply on a fiberglass surface with a 10-pps laser which delivers an average residual energy of 5 J/cm^2 per pulse in approximately 2.5. s.

Acknowledgments

This work was sponsored by U.S. Army High-Energy Laser Systems Project under Contract DAAK40-79-C-0109. The contract monitor was T. E. Norwood. The authors wish to express their appreciation to A. N. Pirri for helpful comments and to M. Staniewicz for the numerical computations.

References

[1] Pirri, A. N., Schlier, R., and Northam, D., "Momentum Transfer and Plasma Formation above a Surface with a High-Power CO_2 Laser," *Applied Physics Letters*, Vol. 21, Aug. 1972, pp. 79-81.

[2] Pirri, A. N., Root, R. G., and Wu, P.K.S., "Plasma Energy Transfer to Metal Surfaces Irradiated by Pulsed Laser," AIAA Paper 77-658, Albuquerque, N. Mex., June 1977.

[3] Wu, P. K. and Nebolsine, P. E., "Laser-Induced to a Phenolic Surface," *AIAA Journal*, Vol. 16, Oct. 1978, pp. 1101-1102.

[4] Vincenti, W. G. and Kruger, Jr., C. H., *Introduction to Physical Gas Dynamics*, Wiley, New York, 1965, p. 463.

[5] Tong, H. and Suchsland, K. E., "Material Response to High-Intensity Laser Radiation," Aerothem Division, Acurex Corp., Mountain View, Calif., Final Rept., Aerotherm Project 6181, Jan. 1972.

[6] Weber, G. A. and Bartle, R. R., "Thermal Design Properties Handbook," AVCO/MSC, Wilmington, Mass., KHDR-AVMSD-68-3, May 1968.

[7] Root, R. G., Pirri, A. N., Wu, P.K.S., and Gelman, H., "Analysis of Laser Target Interaction, Vol. 1—Theory," Physical Sciences Inc., Woburn, Mass., PSI TR-170, March 1979.

J80-164

Proportional Optimal Orthogonalization of Measured Modes

00032
00033
00006

Menahem Baruch*
Technion-Israel Institute of Technology, Haifa, Israel

Introduction

METHODS for orthogonalization of measured mode shapes have been proposed in the literature by several authors.[1-9] In Refs. 9-11, the orthogonalized modes and their measured frequencies were used to correct a given stiffness matrix. In Ref. 10, the present author proposed a method by which the rigid body modes are not corrupted, and the measured credibility of the different groups of measured modes is incorporated by the order of their selection during the orthogonalization process. In fact, Ref. 10 tries to satisfy the seemingly opposed opinions of Rodden[12] and Targoff.[13] Rodden[12] requires the orthogonalization method to keep the rigid body modes uncorrupted and to assign a higher credibility to the measurements of lower-frequency modes, while Targoff[5] thinks that modes which occur in grouping with narrow frequency band must be equally treated. However, the selective method proposed in Ref. 10 satisfies the first or second requirements in a discrete way which cannot be easily controlled. By the method presently proposed,[14] the requirements can be satisfied smoothly and in a controllable way. The different requirements can be satisfied in a simple way by introducing a properly chosen matrix of proportionality. In this way, the corrupted mode shapes are obtained simultaneously. In the numerical example, given "measured" modes are orthogonalized by applying the two methods. The results show clearly the advantages of the presently proposed method. It is interesting to show the relationship among the proposed methods and those of McGrew[3] and Targoff.[8] The selective method degenerates to the McGrew method when the shape modes are selected for orthogonalization one by one. If one chooses the matrix of proportionality to be the unit matrix and orthogonalizes simultaneously all mode shapes, including the rigid body modes, the proportional method[14] degenerates to that of Targoff.[13]

Formulation of the Problem and Its Solution

Following the modified method[10] of the basic approach given in Ref. 9, one must first select the rigid body mode shapes. This must be done in order to keep these modes uncorrupted. Let $R(n \times r)$ be a matrix which represents the analytically known rigid body mode shapes which have already been orthogonalized. Hence,

$$R^t M R = I \tag{1}$$

where $M(n \times n)$ is a known symmetric positive definite mass matrix.

Let $T(n \times q)$ be a matrix which represents the modes which have to be orthogonalized. It must be noted[9,10] that the measured modes $\tilde{T}_i$ have to be normalized in the following way

$$T_i = \tilde{T}_i (\tilde{T}_i^t M \tilde{T}_i)^{-1/2} \tag{2}$$

where $\tilde{T}_i$ is the mode shape before normalization.

Received Feb. 27, 1979; revision received Dec. 17, 1979.

Index categories: Structural Dynamics; Testing, Flight and Ground; Vibration.

*Professor, Dept. of Aeronautical Engineering. Member AIAA.